On the growth and properties of high quality single crystals of the yttrium doped strontium cobaltates, $Y_{1-x}Sr_xCoO_{3-\delta}$ ($0.7 \leq x \leq 0.95$)

C. L. Fleck,* G. Balakrishnan and M. R. Lees

Received 17th August 2010, Accepted 27th October 2010
DOI: 10.1039/c0jm02711a

High quality single-crystals of the A-site and oxygen vacancy ordered variant of yttrium-doped strontium cobaltates $Y_{1-x}Sr_xCoO_{3-\delta}$ ($0.7 \leq x \leq 0.95$) have been produced *via* the floating zone technique. These materials have been the subject of recent research because of their potential applications in solid state devices and for the unusual sensitivity of their magnetic and transport properties to oxygen content. Initial characterisation measurements show the magnetic susceptibility is nearly isotropic and indicative of a weak ferromagnetic response. The large single crystals we have produced are ideal for experiments with the microscopic probes necessary to understand the true nature of the structural and magnetic properties of these compounds.

1. Introduction

The perovskite cobaltates, like the manganites and cuprates, have been found to exhibit a rich variety of interesting physics, including insulator-metal transitions, competition between ferromagnetic and antiferromagnetic exchange, giant magnetoresistance and anomalously high thermopower.[1] In contrast to the cuprates and manganites, the addition of the spin-state degree of freedom makes the cobaltates the archetypal systems for the study of the interplay between the spin, orbital and charge degrees of freedom. In the classic compound $LaCoO_3$, there is a spin-state transition at 100 K,[2] whose precise nature has been the subject of much recent experimental and theoretical work (work on cobaltates has been summarised in a recent review[1]).

In order to manipulate the properties of the perovskite cobaltates such as $SrCoO_3$, recent research has focused on doping where the Sr is replaced with various rare-earth elements (Y, Ho, Er, Dy and Gd[3–7]). In many cases these doped systems have properties that make them particularly suitable for applications compared to their undoped counterparts, such as in fuel cells and membranes for gas separation.[8] The $Y_{1-x}Sr_xCoO_{3-\delta}$ (YSCO) series is one such example,[9] with technologically relevant properties such as high thermopower[10] and increased oxygen diffusion.[11]

YSCO also has the highest ferromagnetic ordering temperature, (T_c = 335 K), of any of the perovskite cobaltates[12] and much of the research on YSCO to date has focused on understanding the competition between the ferromagnetic and the antiferromagnetic exchange interactions in the compound.[13] Neutron diffraction measurements have characterised YSCO as a G-type antiferromagnet[14] and have found no evidence for long-range ferromagnetic ordering. However, laboratory magnetisation measurements on YSCO have detected a ferromagnetic signal, suggesting some short-range or weak ferromagnetic magnetic ordering that may not be representative of the bulk of the material.[15] There is some discussion in the literature as to whether orbital ordering, canting, or a clustering mechanism is responsible for this observed behaviour. The nature of the magnetic order in YSCO is highly dependent on oxygen stoichiometry, and a change in oxygen content of $\Delta\delta = 0.04$ can result in a change from an insulating antiferromagnet to a metallic ferromagnet.[10]

The Y and Sr atoms in $Y_{1-x}Sr_xCoO_{3-\delta}$ occupy the A-site in the ABO_3 perovskite structure. It is possible to prepare both A-site ordered (AO) and A-site disordered (AD) variants of YSCO.[16] In the AO phase, the Y and Sr atoms are ordered in the *ab* plane and CoO_4 tetrahedra alternate with CoO_6 octahedra along the *c* axis. As YSCO forms in such a way that it is oxygen deficient, it is also possible for the oxygen vacancies to be randomly distributed (OD) or for the oxygen vacancies in the CoO_4 layers to order (OO). The fully disordered variant of YSCO (AD/OD) has a simple perovskite structure (Fig. 1 (a)). There then exist two forms of oxygen vacancy ordered YSCO, the AD/OO variant with a brownmillerite crystal structure (Fig. 1 (b)), and the AO/OO variant with a tetragonal crystal structure (Fig. 1 (c)). It is not possible to prepare the AO/OD variant of YSCO. The most interesting of the YSCO structures is the fully-ordered AO/OO variant, which has shown evidence of a complex superstructure, and has variously been claimed to be tetragonal,[17] orthorhombic[18] or monoclinic[5] with no clear consensus in the literature. Magnetically, the AO/OO material also has a T_c = 335 K, more than twice that of the structurally disordered compounds (T_c = 100–150 K).

Recent studies have also established that there is a difference in the charge and spin states of the Co ions in YSCO. The cobalt ions occupying the tetrahedral and octahedral sites have very different values for their magnetic moments.[3] The cobalt ions occupying the tetrahedral sites are in a high spin-state while the cobalt ions on the octahedral sites have an intermediate spin-state. This allows for the possibility of spin-state transitions which have been observed for YSCO under high pressures (~10 GPa)[19] and in high magnetic fields (~53 T).[20]

It is clear from previous work that single crystals would be immensely valuable in understanding the mechanisms governing the structural and magnetic properties of the YSCO system. It is

Physics Department, University of Warwick, Coventry, CV4 7AL, U.K. E-mail: C.L.Fleck@warwick.ac.uk

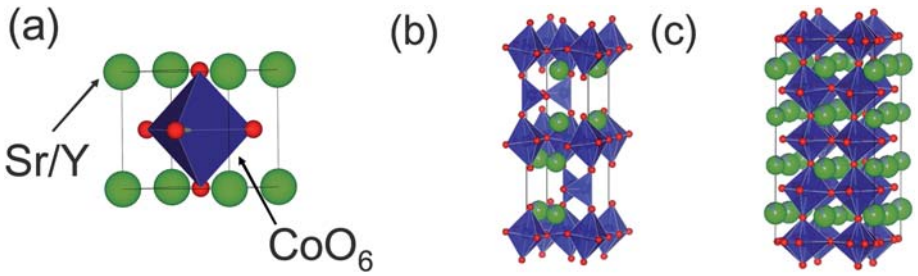

Fig. 1 Crystal structures of (a) AD/OD (space group $Pm\bar{3}m$), (b) AD/OO (space group *Ibm*2) and (c) AO/OO (space group *I*4/*mmm*) forms of $Y_{1-x}Sr_xCoO_{3-\delta}$ ($0.7 \leq x \leq 0.95$) respectively.[16]

known that single crystals of the undoped compound $SrCoO_3$[21,22] can be grown, and a recent paper reported the crystal growth of the $Y_{0.25}Sr_{0.75}CoO_{3-\delta}$ compound.[12] However, the report is very brief and contains a limited discussion of the details of the crystal growth of this series of compounds. In this paper we report the synthesis of high quality crystals of a range of members of the $Y_{1-x}Sr_xCoO_{3-\delta}$ series ($0.7 \leq x \leq 0.95$) and discuss in detail the methods used and the issues associated with the crystal growth. We also present some preliminary characterisation measurements which demonstrate the potential of single crystals to resolve several of the outstanding issues in our understanding of this yttrium-doped strontium cobaltate series and the related rare-earth-doped strontium cobaltates.

2. Sample synthesis and experimental techniques

Polycrystalline samples of $Y_{1-x}Sr_xCoO_{3-\delta}$ were prepared *via* a solid state reaction. High purity powders of $SrCO_3$ (≥99.9%), Y_2O_3 (99.99%), and Co_3O_4 (99.9985%) were mixed together in stoichiometric ratios and sintered in air at 1150 °C for 48 h with intermediate grindings. The resulting materials were then annealed for 24 h at 900 °C in an argon atmosphere to enhance the A-site ordering. Finally, the powders were isostatically pressed into rods of 7–8 mm diameter and 80–90 mm length and annealed at 900 °C for 24 h in an oxygen atmosphere.

Single crystals of $Y_{1-x}Sr_xCoO_{3-\delta}$, with $x = 0.92$, 0.85, 0.8, 0.75 and 0.7, were produced using the floating-zone technique in either a Crystal Systems Incorporated (CSI) four-mirror infrared image furnace or a Nippon Electric Company (NEC) two-mirror image furnace. The growths were performed in a flowing oxygen atmosphere of 3 bars. Initially the seed rod was a polycrystalline rod of the same composition as the feed rod but, for subsequent growths, a seed crystal obtained from the previous growths was used. For the first set of trials, growth speeds of 1–2 mm/h and a rotation rate of 25–30 rpm for both the feed and seed rods were used. For the later experiments, the growth speeds were reduced to 0.5–1 mm/h as it was found that lower growth speeds improved the crystal quality. Crystal facets were visible during the growths. The as-grown crystals were annealed for 24 h at 900 °C in an oxygen atmosphere in order to increase their oxygen content, and the resulting varieties of crystal are hereafter referred to as "O_2-annealed" or "as-grown", as appropriate.

The X-ray Laue method was used to investigate the crystal quality and to align the samples for other experiments. The quality of Laue images taken was limited to some extent by the fluorescence of the cobalt in the samples. Neutron Laue experiments were performed on the OrientExpress Laue diffractometer[23] at the ILL, Grenoble. A Philips PW 1720 X-ray diffraction set with a CuKα source and a monochromating crystal mounted before the detector was used for the X-ray powder diffraction measurements.

The chemical composition of the crystals was determined using thermogravimetric analysis (TGA) and energy dispersive analysis with X-rays (EDAX). A Mettler-Toledo thermal analysis apparatus was used for the TGA. Powdered samples of approximately 30 mg were heated from 30 °C to 900 °C at 10 °C/min in alumina crucibles in a reducing 3% H_2/Ar atmosphere. The change in mass could then be directly related to oxygen loss and therefore the initial oxygen content of the crystals. A JEOL 6100 scanning electron microscope apparatus with an EDAX Genesis option and a thin window detector was used to carry out the EDAX measurements. Several measurements (a minimum of four) were made at different positions on the surface of the crystals. The EDAX measurements gave the average elemental composition of each sample, which were then used to calculate the relative Y/Sr content of the crystals.

In order to measure the magnetic properties of the crystals, small sections were cut from the boules using a low-speed diamond saw. Each boule was encased in wax before cutting to support the material, as the crystals were found to be quite brittle. In some instances the samples were aligned using X-ray Laue method. dc magnetisation measurements as a function of either temperature or applied magnetic field were made between 5 and 400 K in applied magnetic fields of up to 1 T using a Quantum Design SQuID magnetometer. Specific heat measurements were performed on the O_2-annealed crystal using a two-tau relaxation method in a Quantum Design Physical Properties Measurement System (PPMS). The heat capacity of the empty sample stage, together with the grease used to attached the sample to the stage, was subtracted from the measured signal to give the sample heat capacity.

3. Results and discussion

The crystals obtained were around 8 mm in diameter and 30–40 mm in length. Fig. 2 shows the as-grown crystal boules of $Y_{0.15}Sr_{0.85}CoO_{3-\delta}$ and $Y_{0.2}Sr_{0.8}CoO_{3-\delta}$. These are typical of all the crystals grown. The exteriors of the as-grown crystals were a dull grey and X-ray Laue diffraction later showed that this is due to a thin polycrystalline coating covering the interior of the crystals which were clearly shinier and a paler grey. When cutting through the boule, this polycrystalline coating can be easily

Fig. 2 As-grown boules of $Y_{0.15}Sr_{0.85}CoO_{3-\delta}$ (upper panel) and $Y_{0.2}Sr_{0.8}CoO_{3-\delta}$ (lower panel) grown at speeds of 0.5–1 mm/h using the floating-zone method.

distinguished and is usually no more than 0.5 mm thick, although it was observed that increased yttrium doping resulted in a slightly thicker polycrystalline layer.

X-ray diffraction measurements on powdered sections of each boule confirmed the as-grown crystals were the AO/OO variant of YSCO, with the (002) peak characteristic of the *I*4/*mmm* crystal structure[16] clearly visible in the diffraction patterns (see Fig. 3). There was no evidence of any additional peaks in the diffraction patterns, indicating that the crystals are single phase.

An X-ray Laue image taken along the *c* axis of one of the $x = 0.85$ crystals is shown in Fig. 4 (left). Clear diffraction patterns were visible from the cut ends of all the samples produced, indicating that there were indeed single crystals. However, there was evidence from some splitting of the spots that the boules with a higher yttrium content ($x \leq 0.75$) may contain several smaller crystal grains.

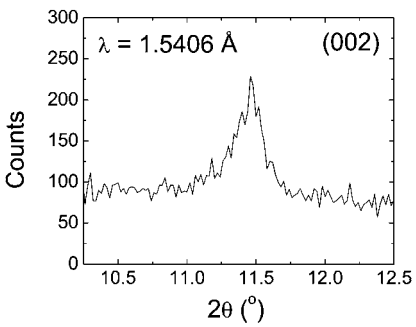

Fig. 3 X-ray diffraction pattern showing the characteristic (002) peak of the AO/OO phase with the *I*4/*mmm* crystal structure as measured on a powdered piece of a $Y_{0.15}Sr_{0.85}CoO_{3-\delta}$ single crystal.

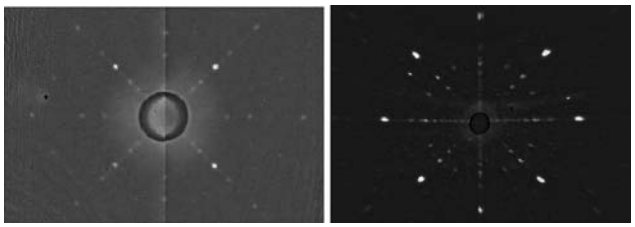

Fig. 4 The left panel shows a typical X-ray Laue back-diffraction image obtained from a crystal of $Y_{0.15}Sr_{0.85}CoO_{3-\delta}$ orientated along the *c* axis. The image was taken on a low voltage setting to avoid excessive cobalt fluorescence. The right panel shows a neutron Laue image along the same axis of the $Y_{0.15}Sr_{0.85}CoO_{3-\delta}$ crystal.

An example of one of the neutron Laue images collected on the OrientExpress Laue diffractometer is shown in Fig. 4 (right). These measurements confirmed that for $0.8 \leq x \leq 0.92$ the quality of the crystals was good, and suitable for further experiments. A 20 mm long, 8 mm diameter section was cut from one crystal boule and found to be a single grain (a later neutron diffraction measurement using a triple-axis spectrometer showed the mosaic spread of this crystal was ~0.7°). A crystal of this volume and quality would be sufficient for experiments requiring large samples, such as inelastic neutron scattering. In contrast, neutron Laue data showed that the samples of a similar volume with $x \leq 0.75$ contained several crystal grains. These measurements support the conclusions made from X-ray Laue measurements, that the boules of $Y_{1-x}Sr_xCoO_{3-\delta}$ with $x = 0.92$, 0.85, and 0.8 are each made up of a large single crystal, while the boules with $x = 0.7$ and 0.75 consist of several smaller crystal grains. The only previous report of single crystals of $Y_{1-x}Sr_xCoO_{3-\delta}$ is for $x = 0.75$.[12] However, the brevity of the report makes it difficult to compare the merits of the method of crystal growth used and the resultant sample quality with the work presented here.

The Y/Sr ratios in the crystals were obtained using EDAX measurements and agree reasonably well with the initial stoichiometries (see Table 1). This indicates that for compounds with $x \geq 0.75$ there is no significant or systematic loss of either strontium or yttrium during the crystal growth process.

An example of one of the reduction curves obtained using TGA is shown in Fig. 5. The stepwise form of the data with two

Table 1 The oxygen content $3 - \delta$ of various members of the as-grown $Y_{1-x}Sr_xCoO_{3-\delta}$ ($0.7 \leq x \leq 0.85$) series determined using TGA. Values of x are given both for the nominal starting stoichiometry and from the EDAX measurements. It should be noted that the error in the experimentally determined value of x is the predominant source of error in calculating the oxygen content of each of the crystals. The cobalt valency has been calculated using charge balance. The values marked with a * correspond to those for the O_2-annealed $x = 0.85$ sample

Y/Sr Composition		Oxygen Content	Co Valency
Nominal Starting	EDAX	$3 - \delta$	
0.15/0.85	0.17(1)/0.83(1)	2.59(1)	3.03(4)
		2.63(1)*	3.11(4)*
0.20/0.80	0.22(1)/0.78(2)	2.61(1)	3.02(4)
0.25/0.75	0.26(1)/0.74(1)	2.57(2)	2.90(6)
0.30/0.70	0.26(1)/0.74(1)	2.53(2)	2.77(6)

intermediate plateaus is typical of the reduction curves for this family of cobalt oxides.[17,24] The reduction of YSCO to its constituent oxides is completed around 800 °C. The change in mass gives us the oxygen loss during the process. The values obtained using this method, given in Table 1, show a decrease in oxygen content for crystals with higher yttrium doping.

An $Y_{1-x}Sr_xCoO_{3-\delta}$ single crystal with $x = 0.85$ was chosen for a more in-depth study, as the quality of the crystal was good and this value of x is within the doping range necessary for observing a room-temperature ferromagnetic response from the sample.

A comparison between the oxygen content of as-grown and O_2-annealed crystals was also performed using thermogravimetric analysis and the results for the $x = 0.85$ crystal are also shown in Table 1. There is an increase in oxygen content of $\delta = 0.04$ for the O_2-annealed crystal compared to the crystal as-grown. From the value for δ, and assuming the valencies of Sr and Y to be 2+ and 3+ respectively, the cobalt valencies were calculated and are given in Table 1. The cobalt valency was found to be very close to pure trivalent cobalt for the as-grown crystal, but for the annealed crystal these measurements imply the presence of a small amount of tetravalent cobalt.

Powder neutron diffraction measurements have shown that the magnetic order in $Y_{1-x}Sr_xCoO_{3-\delta}$ is antiferromagnetic.[14] However, for both AO/OO and AD/OO powders, dc magnetisation measurements are dominated by a weak ferromagnetic response which does not appear to be representative of the bulk of the sample. The Curie temperature varies according to the oxygen content of the material, and is 100–150 K for A-site disordered material and 330–370 K for A-site ordered material.

Fig. 6 shows the dc magnetic susceptibility *versus* temperature measurements made on as-grown and O_2-annealed crystals of $Y_{0.15}Sr_{0.85}CoO_{3-\delta}$. For the as-grown crystal (see Fig. 6 (a)) the magnetic ordering temperature is 350 K and the magnitude of the magnetisation at 5 K is very low. A broad peak at ~100 K suggests that a small quantity of the AD/OD phase is present.[16] For the O_2 annealed crystal (see Fig. 6 (b)) a transition is clearly observed at 370 K. This (ferromagnetic) transition occurs at the same temperature as that reported for an $x = 0.25$ single crystal[12] and coincides with the bulk antiferromagnetic transition seen in this material by powder neutron diffraction.[14] A second transition is present at 280 K. This feature has been previously observed in dc magnetisation measurements on YSCO powders and is generally attributed to a further weak ferromagnetic transition linked to the range of possible oxygen stoichiometries found in this material.[16] The magnetic response characteristic of the AD/OD material (a change in slope at ~150 K) is also visible in the data. This result suggests that the sample contains around 1% of the AD/OD phase. The increase in the transition temperature of the AD/OD minority phase (as compared to that seen in the as-grown sample) is consistent with an increase in the oxygen content of this phase due to the O_2 annealing. At 5 K the magnetisation signal of the O_2-annealed sample is almost two-orders of magnitude larger than for the as-grown sample.

Fig. 7 shows the dc magnetisation as a function of applied magnetic field for the O_2-annealed crystal. These $M(H)$ curves clearly reveal the ferromagnetic character of the magnetic

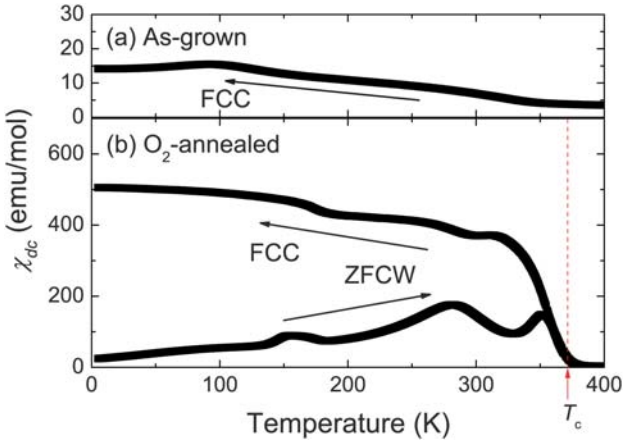

Fig. 6 The temperature dependence of the zero-field cooled warming (ZFCW) and field-cooled cooling (FCC) dc magnetisation of a crystal of $Y_{0.15}Sr_{0.85}CoO_{3-\delta}$. Panel (a) shows the magnetisation for the as-grown crystal with a δ value of 0.41 and panel (b) shows the magnetisation for the O_2-annealed crystal ($H \| c$) with a δ value of 0.37. The measurements were made in an applied magnetic field $\mu_0 H = 0.1$ T.

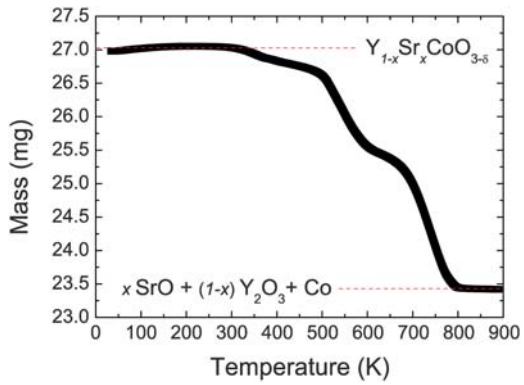

Fig. 5 A typical TGA curve for the reduction of a powdered $Y_{0.15}Sr_{0.85}CoO_{3-\delta}$ crystal in a 3% H_2/Ar atmosphere. This particular measurement was for the O_2-annealed $Y_{0.15}Sr_{0.85}CoO_{3-\delta}$ crystal, but all the measurements for each of the crystals grown showed the same features.

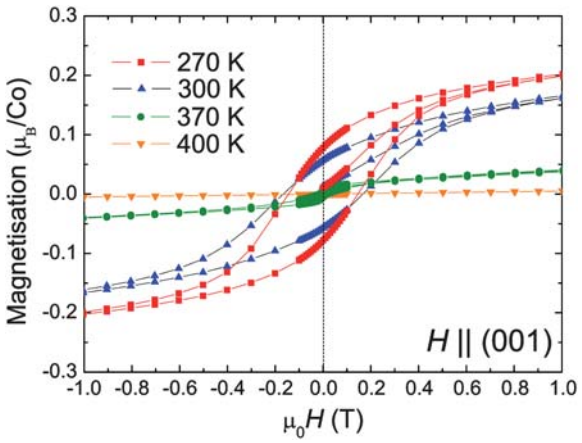

Fig. 7 The field dependence of the dc magnetisation of an O_2-annealed crystal of $Y_{0.15}Sr_{0.85}CoO_{3-\delta}$. The sample was warmed above T_c between runs.

transition seen at 370 K in the $M(T)$ data. As the temperature is reduced from 400 K to 270 K there is a rapid increase in the magnitude of magnetisation which is accompanied by the appearance of hysteresis in the $M(H)$ loops below 370 K, shown in Fig. 7. The coercive field is around 0.2 T below 300 K and the non-saturating component at high fields is suggestive of an antiferromagnetic component to the magnetisation.

Magnetisation measurements made on as-grown and annealed single crystal samples with the magnetic field applied parallel and perpendicular to the c axis reveal that the magnitude of the magnetisation at 7 T (data not shown) is ~5% higher for $H\|c$, indicating that there is a small net magnetic moment aligned along the c axis. On the other hand, given the highly anisotropic crystal structure, the relatively isotropic magnetic response of the materials leaves open the possibility that the ferromagnetic signal is not representative of the magnetic order within the bulk of the samples and that the ferromagnetism is caused by a mechanism such as spin clustering. The TGA measurements for the O_2 annealed crystal suggest the presence of a small amount of Co^{4+}, which would be expected if clustering were the mechanism behind the observed ferromagnetism.[14] Further work is required to fully understand the nature of the magnetic order in $Y_{1-x}Sr_xCoO_{3-\delta}$.

Fig. 8 shows the temperature dependence of the specific heat capacity, $C(T)$, of the O_2-annealed YSCO crystal and the non-magnetic perovskite $LaGaO_3$ that is used to estimate the lattice contribution to the heat capacity. The heat capacity of the YSCO contains only one significant feature corresponding to a bulk transition at $T_c = 370$ K. This means that the entropy associated with the features seen at 150 K and 280 K in the $M(T)$ data is small and may be linked with either spin reorientations within an ordered state, or to some magnetic ordering that occurs in a very small volume fraction of material. The extreme sensitivity of the magnetic properties of YSCO to both oxygen disorder and oxygen concentration suggests the latter is more likely.[16] The total magnetic entropy released between 3 and 420 K[25] is 11.8 J $mol^{-1}K^{-2}$ which is ~88% of the $R\ \ln(2S + 1) =$ 13.4 J mol^{-1} K^{-1} expected for a Co^{3+} ion with a fully quenched orbital moment where $S = 2$ and R is the gas constant. The

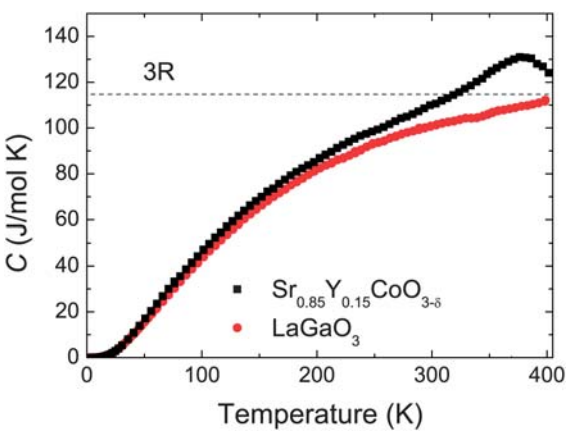

Fig. 8 Temperature dependence of the specific heat of a single crystal of O_2-annealed $Y_{0.15}Sr_{0.85}CoO_{3-\delta}$. $LaGaO_3$, a non-magnetic perovskite, was also measured and is shown for comparison. The horizontal line indicates the value of $3R$ per atom for YSCO.

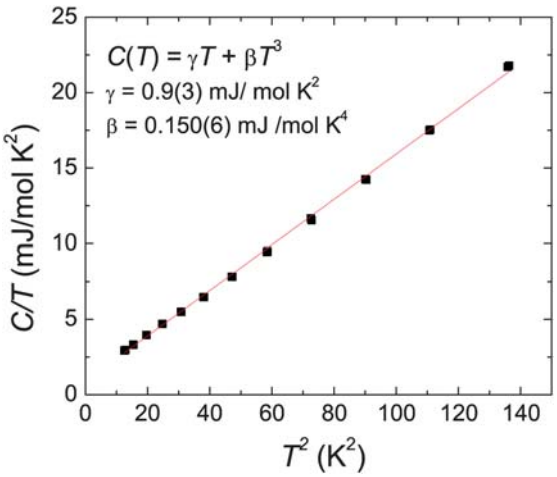

Fig. 9 C/T vs T^2 for the low temperature specific heat ($2 < T < 12$ K) of a single crystal of O_2-annealed $Y_{0.15}Sr_{0.85}CoO_{3-\delta}$. The fit is to a model consisting of the electronic (γT) and the lattice (βT^3) contributions to the specific heat, which is shown to be a good description of the low temperature data.

low-temperature ($T \leq 12$ K) data can be fitted using $C(T) = \gamma T + \beta T^3$ (see Fig. 9). This gives a $\gamma = 0.90$ mJ mol^{-1} K^{-2}, a rather low value that is consistent with previous reports on transition metal oxides that are close to the boundary between an insulating antiferromagnetic and a metallic ferromagnet state.[26–28] Using β we calculate the Debye temperature $\theta_D = \left(\frac{12}{5}\pi^4 pR/\beta\right)^{1/3}$ where p is the number of atoms in each molecule giving $\theta_D =$ 391 K, a result that is compatible with the data at higher temperatures. Adding contributions that vary as T^n with $n = 3/2$ or 2 does not improve the quality of the fits suggesting that any magnetic spin-wave contribution to C varies as T^3, a behaviour that is typical for a bulk antiferromagnet and consistent with the arguments presented earlier.

4. Conclusions

Single crystals of $Y_{1-x}Sr_xCoO_{3-\delta}$ with $0.7 \leq x \leq 0.95$ have been grown using the floating-zone method. The crystals with $x \geq 0.80$ were found to be of high quality. X-ray and neutron Laue methods have shown that crystals with volumes of at least 1 cm^3 can be prepared. It is possible that lightly-doped single crystals of the entire $R_{1-x}Sr_xCoO_{3-\delta}$ (where R = Ho, Er, Dy,…) family of materials can be grown using this method. The crystals produced are suitable for most physical property measurements and examples of magnetisation and specific heat measurements have been presented.

The single crystals of YSCO grown in this study form with the AO/OO structure, as demonstrated by the presence of the (002) peak, characteristic of the $I4/mmm$ crystal structure, in the powder X-ray diffraction patterns. As-grown and O_2-annealed crystals of $Y_{0.15}Sr_{0.85}CoO_{3-\delta}$ were characterised using dc magnetisation and specific heat measurements. The results agree well with previous reports for polycrystalline samples and confirm that the materials are suitable for further in-depth studies. The dc

magnetisation measurements show a nearly isotropic response with a small net magnetic moment along the *c* axis.

Previous work on the YSCO family of materials make it clear that high quality single crystals of these materials are needed in order to fully understand the complex structural and magnetic behaviour of these compounds. The ambiguities in the literature regarding the structure[9,17,18] can be most convincingly resolved *via* detailed single-crystal X-ray diffraction studies. Understanding the true nature of the magnetic order and the interplay between ferromagnetic and antiferromagnetic interactions within this material requires single-crystal neutron studies. Measurements on single crystals that address these issues are now under way.

The authors would like to the thank the EPSRC, UK for funding of the crystal growth programme (EP/I007210/1). Some of the equipment used in this research was obtained through Birmingham Science City: Creating and Characterising the Next Generation Advanced Materials, with support from Advantage West Midlands (AWM) and part funded by the European Regional Development Fund (RDF). The VESTA software package[29] was used in the drawing of Fig. 1.

References

1 N. B. Ivanova, S. G. Ovchinnikov, M. M. Korshunov, I. M. Eremin and N. V. Kazak, *Phys.-Usp.*, 2009, **52**, 789.
2 A. Podlesnyak, S. Streule, J. Mesot, M. Medarde, E. Pomjakuushina, K. Conder, A. Tanaka, M. W. Haverkort and D. I. Khomskii, *Phys. Rev. Lett.*, 2006, **97**, 247208.
3 D. V. Sheptyakov, V. Yu. Pomjakushin, O. A. Drozhzhin, S. Ya. Istomin, E. V. Antipov, I. A. Bobrikov and A. M. Balagurov, *Phys. Rev. B: Condens. Matter Mater. Phys.*, 2009, **80**, 024409.
4 S. Balamurugan, K. Yamaura, A. Asthana, A. Ubaldini, Y. Matsui and E. Takayama-Muromachi, *J. Appl. Phys.*, 2008, **103**, 07B903.
5 S. Ishiwata, W. Kobayashi, I. Terasaki, K. Kato and M. Takata, *Phys. Rev. B: Condens. Matter Mater. Phys.*, 2007, **75**, 220406(R).
6 A. Hassen, A. I. Ali, B. J. Kim, Y. S. Wu, S. H. Park and Bog G. Kim, *J. Appl. Phys.*, 2007, **102**, 123905.
7 Y. F. Zhang, S. Sasaki, O. Yanagisawa and M. Izumi, *J. Magn. Magn. Mater.*, 2007, **310**, 1002.
8 K. Zhang, R. Ran, L. Ge, Z. Shao, W. Jin and N. Xu, *J. Alloys Compd.*, 2009, **474**, 477.
9 S. Ya. Istomin, J. Grins, G. Svensson, O. A. Drozhzhin, V. L. Kozhevnikov, E. V. Antipov and J. P. Attfield, *Chem. Mater.*, 2003, **15**, 4012.
10 A. Maignan, S. Hebert, V. Caignaert, V. Pralong and D. Pelloquin, *J. Solid State Chem.*, 2005, **178**, 868.
11 D. Rupasov, A. Chroneos, D. Parfitt, J. A. Kilner, R. W. Grimes, S. Ya. Istomin and E. V. Antipov, *Phys. Rev. B: Condens. Matter Mater. Phys.*, 2009, **79**, 172102.
12 W. Kobayashi and I. Terasaki, *AIP Conf. Proc.*, 2006, **850**, 1223.
13 W. Kobayashi, S. Ishiwata, I. Terasaki, M. Takano, I. Grigoraviciute, H. Yamauchi and M. Karppinen, *Phys. Rev. B: Condens. Matter Mater. Phys.*, 2005, **72**, 104408.
14 D. J. Goossens, K. F. Wilson, M. James, A. J. Studer and X. L. Wang, *Phys. Rev. B: Condens. Matter Mater. Phys.*, 2004, **69**, 134411.
15 S. Fukushima, T. Sato, D. Akahoshi and H. Kuwahara, *J. Appl. Phys.*, 2008, **103**, 07F705.
16 S. Fukashima, T. Sato, D. Akahoshi and H. Kuwahara, *J. Phys. Soc. Jpn.*, 2009, **78**, 064706.
17 M. James, D. Cassidy, D. J. Goossens and R. L. Withers, *J. Solid State Chem.*, 2004, **177**, 1886.
18 M. James, M. Andeev, P. Barnes, L. Morales, K. Wallwork and R. L. Withers, *J. Solid State Chem.*, 2007, **180**, 2233.
19 N. O. Golosova, D. P. Kozlenko, L. S. Dubrovinsky, O. A. Drozhzhin, S. Ya. Istomin and B. N. Savenko, *Phys. Rev. B: Condens. Matter Mater. Phys.*, 2009, **79**, 104431.
20 S. Kimura, Y. Maeda, T. Kashiwagi, H. Yamaguchi, M. Hagiwara, S. Yoshida, I. Terasaki and K. Kindo, *Phys. Rev. B*, 2008, **78**, 180403(R).
21 H. Takei, H. Oda, H. Watanabe and I. Shindo, *J. Mater. Sci.*, 1978, **13**, 519.
22 A. Nakatsuka, A. Yoshiasa, N. Nakayama, T. Mizota and H. Takei, *Acta Crystallogr., Sect. C: Cryst. Struct. Commun.*, 2004, **60**, i59.
23 B. Ouladdiaf, J. Archer, G. J. McIntyre, A. W. Hewat, D. Brau and S. York, *Phys. B*, 2006, **385–386**, 1052.
24 M. Karppinen, M. Matvejeff, K. Salomaki and H. Yamauchi, *J. Mater. Chem.*, 2002, **12**, 1761.
25 The heat capacity data for YSCO between 400 and 420 K was extrapolated from the measurements below 400 K in order to calculate the point of intersection with the $LaGaO_3$ data.
26 B. F. Woodfield, M. L. Wilson and J. M. Byers, *Phys. Rev. Lett.*, 1997, **78**, 3201.
27 M. R. Lees, O. A. Petrenko, G. Balakrishnan and D. McK. Paul, *Phys. Rev. B*, 1999, **59**, 1298.
28 C. He, S. Eisenberg, C. Jan, H. Zheng, J. F. Mitchell and C. Leighton, *Phys. Rev. B: Condens. Matter Mater. Phys.*, 2009, **80**, 214411.
29 K. Momma and F. Izumi, *J. Appl. Crystallogr.*, 2008, **41**, 653.